# Spin equilibrium in strongly magnetized accreting stars

## C. R. D'Angelo★

*Leiden Observatory, Leiden University, Postbus 9513, NL-2300 RA Leiden, The Netherlands*

## ABSTRACT

Strongly magnetized accreting stars are often hypothesized to be in 'spin equilibrium' with their surrounding accretion flows, which requires that the accretion rate changes more slowly than it takes the star to reach spin equilibrium. This is not true for most magnetically accreting stars, which have strongly variable accretion outbursts on time-scales much shorter than the time it would take to reach spin equilibrium. This paper examines how accretion outbursts affect the time a star takes to reach spin equilibrium and its final equilibrium spin period. I consider several different models for angular momentum loss – either carried away in an outflow, lost to a stellar wind, or transferred back to the accretion disc (the 'trapped disc'). For transient sources, the outflow scenario leads to significantly longer times to reach spin equilibrium ($\sim 10 \times$), and shorter equilibrium spin periods than would be expected from spin equilibrium arguments, while the 'trapped disc' does not. The results suggest that disc trapping plays a significant role in the spin evolution of strongly magnetic stars, with some caveats for young stellar objects.

**Key words:** accretion, accretion discs – MHD – stars: neutron – stars: magnetic field – stars: protostars – stars: rotation.

## 1 INTRODUCTION

The spin rate of a star is strongly affected by the presence of a magnetic field. Neutron stars (NSs), for example, show a clear inverse correlation between magnetic field strength and spin rate: the fastest millisecond pulsars ($P_{\rm spin} \sim 0.002$–$0.005$ s) have typical field strength of $B \sim 10^8$ G, while magnetars with $B \sim 10^{14}$ G have typical spin periods of a few seconds. The influence of the magnetic field is even stronger when such stars are accreting gas. Although accreted gas adds considerable angular momentum to the star, accreting magnetized stars generally spin well below their breakup velocity (sometimes many orders of magnitude slower), indicating that the presence of the magnetic field is able to regulate the transport of angular momentum between the star and surrounding gas.

The stellar magnetic field in fact strongly affects the dynamics of the accreting gas, and couples the star to its surrounding environment. Close to the star, matter is forced to flow along field lines on to the magnetic poles. At the boundary of this region (typically called the *magnetospheric* or *Alfvén radius*, $r_{\rm m}$), the magnetic field can in turn be significantly distorted by the gas, which exerts a torque on the star. The sign of the torque depends on the relative location between $r_{\rm m}$ and the *corotation radius*, $r_{\rm c} \equiv (GM/\Omega_*^2)^{1/3}$, or the location where a Keplerian disc corotates with the star. If $r_{\rm m} > r_{\rm c}$, the star spins faster than the inner disc, so that field lines coupling the two will gradually spin-down the star. The location of the magnetospheric radius itself is chiefly determined by the stellar magnetic field and accretion rate, although it is also sensitive to the detailed interaction between the gas and the magnetic field.

This basic picture leads naturally to the concept of 'spin equilibrium' (or 'disc locking' in young stars), whereby the star's spin rate gradually adjusts itself until the net torque on the star is roughly zero and the accretion flow is truncated near the corotation radius, $r_{\rm m} \simeq r_{\rm c}$. In this way, the star's dipolar magnetic field can be estimated, provided the spin and accretion rate are known. Assuming spin equilibrium is reached requires assuming a steady mass accretion rate – i.e. that the time-scale on which the accretion rate changes is generally much longer than the 'spin-equilibrium time' ($T_{\rm eq}$), defined as the time the star takes to reach its 'spin-equilibrium period' ($P_{\rm eq}$).

It is not clear that this assumption is widely valid for accreting magnetized stars, either compact stars (magnetized white dwarfs and NSs) or young stellar objects (YSOs). Most magnetized compact stars in binary systems are transient, showing short accretion outbursts followed by long periods of quiescence. In weak-field accreting NSs, the low-mass X-ray binaries (LMXBs), the observed duty cycle is on average 3 per cent, but can be well below 1 per cent when allowing for the limited observing baseline (Yan & Yu 2015). The luminosity difference in LMXBs between outburst and quiescence can span many orders of magnitude, suggesting a huge change in accretion rate. High magnetic field transient NSs can also show strong variability. In one particular class of system, Be X-ray binaries (NSs that accrete from the wind or disc surrounding a Be star), the duty cycles are $\sim 5$–$20$ per cent (Reig 2011; Klus et al. 2014),

★ E-mail: dangelo@strw.leidenuniv.nl

and the dynamic range can be 1–5 orders of magnitude between outburst and quiescence.

At least some YSOs also show large-scale variability, but its prevalence is much harder to constrain, since they evolve on much longer time-scales than compact binaries. The most dramatic accretion outbursts are FU Ori-type outbursts, where the luminosity increases by ∼1000 (Hartmann & Kenyon 1996), with an outburst duration of at least decades and recurrence time of several thousand years. Strong luminosity variations of about 1–2 orders of magnitude on shorter (years) time-scales are also sometimes seen (the 'EXor' class; Audard et al. 2014, suggesting that the mean accretion rate can vary considerably at different points in the TTauri phase.

Variations in accretion rate may help explain observations in magnetospherically accreting systems that do not easily fit into the standard spin-equilibrium picture. YSOs with discs, for example, show clear indications of magnetic field regulated rotation, spinning well below their breakup values. However, attempts to confirm disc locking have been mixed, or seemed to contradict simple model predictions (Cauley et al. 2012). To give another example, a recent survey of the spin rates in Be X-ray binaries found that the NS frequently rotates much more slowly than would be expected for a moderate ($10^{12}$ G) magnetic field star in spin equilibrium, suggesting that much larger fields ($10^{14}$–$10^{15}$ G) are present (Klus et al. 2014). The large number of such binaries makes this unlikely from a population point of view, and it also seems to contradict magnetic field estimates from cyclotron lines in analogous Galactic systems with similar spin rates and luminosities (Ho et al. 2014).

This paper investigates how large-amplitude, short-time-scale accretion rate variations affect the spin evolution of the star, and how this evolution changes for different models for stellar angular momentum loss. As described in more detail below, it is not clear whether most angular momentum is lost through stellar outflows (winds from the star, or at the disc–magnetic field interface) or whether angular momentum is mainly lost to the accretion disc. As I demonstrate below, different angular momentum loss mechanisms lead to different predictions for spin evolution as a function of accretion rate, so that comparing the long-term spin evolution of each model with different accretion rate profiles may offer new observational tests to distinguish between them.

## 2 MODELS FOR MAGNETOSPHERIC ACCRETION

The basic picture for how a strong stellar magnetic field interacts with accreting gas is theoretically fairly well established and supported by numerical magnetohydrodynamical (MHD) simulations, although there are still some significant uncertainties (see e.g. Uzdensky 2004 or Lai 2014 for theoretical reviews).

In the region closest to the star, the magnetic field completely determines the gas behaviour, truncating the accretion disc at the magnetospheric radius, $r_{\rm m}$. The field lines in this inner region remain closed and infalling gas flows along the field lines to accrete near the magnetic poles of the star. Just outside $r_{\rm m}$, field lines couple to the disc, and this coupling exerts a torque on the star due to the differential rotation between the disc and the star, which twists magnetic field lines and generates a toroidal field component. In the low-density atmosphere above the disc, 'force-free' conditions apply, meaning that the increasing magnetic pressure (from the generated toroidal field component) causes magnetic field lines to inflate and eventually open up, potentially driving an outflow from the disc (e.g. Goodson, Winglee & Boehm 1997; Miller & Stone 1997). Some open field lines may subsequently reconnect,

and small-scale instabilities at the interface between the disc and the closed magnetosphere can recouple the star and the disc, starting the cycle again.

The resulting global field geometry is significantly different from early suggestions (e.g. Ghosh, Pethick & Lamb 1977; Ghosh & Lamb 1979; hereafter GL) in that only a small region at the inner edge of the disc is coupled to the magnetic field ($\Delta r/r < 1$). In contrast the GL model proposed that stellar magnetic field lines remain embedded over a wide radial extent in the disc, so that large amounts of angular momentum are transported to the disc through the twisting of the field lines. This was shown to be physically inconsistent by Wang (1987), since the high level of twist proposed by this model would be enough to completely disrupt the outer disc. Later work (e.g. Aly & Kuijpers 1990; Lovelace, Romanova & Bisnovatyi-Kogan 1995; Hayashi, Shibata & Matsumoto 1996) demonstrated that field lines will tend to become open, so that only the inner edge of the disc is coupled to the star.

All accreting magnetic stars are generically observed to spin well below their breakup frequencies, some (e.g. some NSs with Be star or giant companions) up to six orders of magnitude more slowly. As the star accretes from the truncated disc, the angular momentum in the gas will be added to the star and make it spin faster, but how the star sheds angular momentum remains uncertain. MHD simulations tend to show strongly time-dependent accretion and outflows that carry away angular momentum, although the details remain simulation dependent (compare e.g. Zanni & Ferreira 2013; Lii et al. 2014). Simulations can also show strongly distorted field lines around the rotation axis, which carry away a significant amount of angular momentum from the star. Angular momentum can also be deposited directly into the accretion disc, changing its structure (see Section 2.4; Sunyaev & Shakura 1977; D'Angelo & Spruit 2010), or be removed via a wind from the stellar surface (Section 2.3; Matt & Pudritz 2005).

### 2.1 Location of magnetospheric radius

The location of the disc's inner edge can be estimated from the accretion rate and the star's magnetic field and mass. For the simple case in which gas accretes radially on to the star, $r_{\rm m}$ is estimated by setting the ram pressure of the infalling gas $\rho \upsilon^2$ equal to the magnetic pressure of the dipolar magnetic field $B^2/8\pi$. In terms of the mass accretion rate, this leads to a 'standard' expression for $r_{\rm m}$ (Pringle & Rees 1972):

$$r_{\rm m,0} = \mu^{4/7} \dot{M}^{-2/7} (2GM_*)^{-1/7}, \tag{1}$$

where $\dot{M}$ is the accretion rate through the inner regions of the disc, $\mu = B_* R_*^3$ is the magnetic moment of the star, and $M_*$ is its mass. For accretion from a circumstellar disc, the thinness of the disc and the Keplerian rotation makes it more difficult for the magnetic field to force the gas into corotation with the star, so that $r_{\rm m}$ is smaller than for the radial-infall case (e.g. Ghosh & Lamb 1979; Wang 1987); $r_{\rm m} = \xi r_{\rm m,0}$; $\xi < 1$. In this case, $r_{\rm m}$ is very sensitive to the details of the coupling between the accretion disc and magnetic field, which is the most uncertain aspect of the problem. Various revised theoretical estimates for $r_{\rm m}$ have been proposed, suggesting $\xi \sim 0.5$–1 (e.g. Ghosh et al. 1977; Spruit & Taam 1993; hereafter ST93,Wang 1996; Kluźniak & Rappaport 2007; Bessolaz et al. 2008).

Wang (1987) suggested a slightly different approach in estimating $r_{\rm m}$ in a disc by imposing conservation of angular momentum flux across $r_{\rm m}$. This is most significant when the rotation rate of the inner disc is close to the star's rotation rate. Using this estimate

gives a slightly different expression from equation (1), and explicitly incorporates the star's rotation frequency, $\Omega_*$:

$$r_{\mathrm{m}} = \left(\frac{\eta}{4}\right)^{1/5} \mu^{2/5} \Omega_*^{-1/5} \dot{M}^{-1/5}. \tag{2}$$

Here, $\eta = B_\phi/B_{\mathrm{r}} < 1$ is the magnitude of the toroidal magnetic field, $B_\phi$ generated by twisting magnetic field lines through differential rotation between the star and the disc. For $r_{\mathrm{m}} = r_{\mathrm{c}}$, equation (2) reduces to equation (1) with $\xi \sim 0.4$–$0.7$ (for $\eta = 0.1$–$1$). Although the location of $r_{\mathrm{m}}$ is only uncertain by a factor of a few, the strong dependence of $\dot{M}$ on $r_{\mathrm{m}}$ means that the *accretion rate* for which $r_{\mathrm{m}} = r_{\mathrm{c}}$ (i.e. when spin equilibrium is reached) can be uncertain by up to $\xi^{-7/2} = 300 \times$.

The geometrical structure of the accretion disc can also affect the location of $r_{\mathrm{m}}$. At very low or high accretion rates, the standard 'thin disc' accretion solution (Shakura & Sunyaev 1973) likely does not apply, and the flow becomes a geometrically thick radiatively inefficient accretion flow (RIAF, such as the Advection Dominated Accretion Flow solution; Narayan & Yi 1994). An RIAF rotates with significantly sub-Keplerian velocities and is much less dense than a thin disc at the same accretion rate. This means that for the same accretion rate, the magnetospheric radius will likely be larger for an RIAF than a thin disc. This suggests that a significant change in accretion flow structure and geometry may be accompanied by a large change in $r_{\mathrm{m}}$ even without changing $\dot{M}$, which could have a strong observational effect. Additionally, since the accreted gas is considerably sub-Keplerian and geometrically thick, the angular momentum exchange between the flow and the star could be considerably altered, driving stronger outflows, for example or enhancing the spin-down rate of the star. The interaction between an RIAF and a magnetic field has not been studied in detail, but is likely very relevant both for LMXBs at low luminosity and NSs accreting at super-Eddington rates, such as the recently discovered pulsars in ultraluminous X-ray binaries (Bachetti et al. 2014; Fürst et al. 2016).

## 2.2  Standard accretion/ejection model

The simplest model for angular momentum loss proposes that infalling gas (and its angular momentum, $\sim \dot{M}\Omega_K(r_{\mathrm{m}})r_{\mathrm{m}}^2$) is either accreted on to the star (when $r_{\mathrm{m}} < r_{\mathrm{c}}$) or ejected in an outflow (when $r_{\mathrm{m}} > r_{\mathrm{c}}$). If all the specific angular momentum of the gas is either accreted or expelled, the rate of angular momentum change in the star (i.e. the angular momentum of the accreting gas, using equation (1) for the location of $r_{\mathrm{m}}$) is given by:

$$\dot{J} = 2^{-1/14} \xi^{1/2} \dot{M}^{6/7} \mu^{2/7} (GM_*)^{3/7} \tanh\left(\frac{r_{\mathrm{m}} - r_{\mathrm{c}}}{\Delta r_2}\right). \tag{3}$$

Here, the tanh function and the parameter $\Delta r_2$ are introduced to move smoothly between the two solutions (ejection versus accretion). Simulations typically show that the transition between accretion and strong outflow occurs across a wide range of accretion rates (which sets $r_{\mathrm{m}}$), so that there are a range of accretion rates that show both accretion and ejection (e.g. Romanova et al. 2003). By introducing $\Delta r_2$, I can systematically investigate how the size of this transition length-scale affects the final equilibrium spin period and spin-down time of the star (see also in Section 4.3).

Some simulations (e.g. Zanni & Ferreira 2013) show very energetic outflows, in which matter is ejected well above its escape velocity, so that rate of angular momentum loss is larger than $\sim \dot{M}_{\mathrm{ej}}(GMr_{\mathrm{m}})^{1/2}$ (where $\dot{M}_{\mathrm{ej}}$ is the mass-loss rate of the outflow). This will increase the equilibrium $\dot{M}$ (the accretion rate where

$r_{\mathrm{m}} = r_{\mathrm{c}}$ since more gas will reach the stellar surface without spinning up the star. These simulations also show mass ejections even during phases dominated by accretion, demonstrating that there can be significant angular momentum lost from the star even during accretion phases. The increase in the equilibrium $\dot{M}$ can be approximated by changing $\xi$ in equation (1). For simplicity however, I make the explicit assumption that in the limit $r_{\mathrm{m}} \gg r_{\mathrm{c}}$ (the strong propeller regime), the outflow of angular momentum is limited by $\dot{M}_{\mathrm{ej}}(GMr_{\mathrm{m}})^{1/2}$.

In equation (3) and throughout this paper, the accretion rate $\dot{M}$ refers to the amount of gas accreting through the inner regions of the disc. If most of this gas is ejected, the net accretion rate on to the star will naturally be much lower. For a disc magnetically truncated at more than a few stellar radii from the star, the stellar accretion rate largely determines the accretion luminosity, so it is somewhat difficult to define the accretion rate through the disc without an accretion model: is their low luminosity because most of the gas is begin expelled (the ejection scenario) or because the accretion rate is intrinsically low but accretion continues fairly efficiently (the trapped disc scenario outlined in Section 2.4).

## 2.3  Spin regulation by a stellar wind

It has also been suggested (specifically for young stars) that angular momentum could be lost from a stellar wind powered by accretion energy (Matt & Pudritz 2005). As described by Matt & Pudritz (2005), the angular momentum loss to the wind is given by:

$$\dot{J} = -\dot{M}_{\mathrm{w}}\Omega_* r_{\mathrm{A}}^2, \tag{4}$$

where $\dot{M}_{\mathrm{w}}$ is the mass-loss rate in the wind, and $r_{\mathrm{A}}$ is defined as the location where the wind speed equals that of magnetic Alfvén waves:

$$r_{\mathrm{A}} \sim R_* K \left(\frac{\mu^2}{\dot{M}_{\mathrm{w}} \upsilon_{\mathrm{esc}} R_*}\right)^m. \tag{5}$$

Here, $K \sim 2.1$ and $m \sim 0.2$ are fit constants from MHD simulations and $\upsilon_{\mathrm{esc}}$ is the escape speed at the stellar surface (Matt & Pudritz 2008). The distinction in terms of angular momentum loss between this and the accretion/ejection picture is that here the star is assumed to efficiently lose angular momentum to the wind at all accretion rates, instead of only when there is a significant centrifugal barrier (i.e. $r_{\mathrm{in}} > r_{\mathrm{c}}$).

Whether a wind can efficiently carry away angular momentum thus depends largely on the amount of mass loss in the wind (assuming it is launched not far above its escape velocity). YSOs are observed to have outflows of up to $\sim 10$ per cent of $\dot{M}$ for protostellar systems (Matt & Pudritz 2005), but it is difficult to tell whether this outflow originates from the star or the inner disc. The ability of a stellar wind to efficiently carry away enough angular momentum to regulate YSO spins has further been challenged by Zanni & Ferreira (2011). I assume in this paper that a wind acts in conjunction with the accretion/ejection model, so that at low $\dot{M}$ there are two sources of angular momentum loss: from the wind and from a centrifugally launched outflow.

## 2.4  Trapped disc model

When the inner edge of the accretion disc lies outside the corotation radius, a centrifugal barrier inhibits accretion on to the star. However, the disc–field interaction may not be strong enough to drive a strong outflow. If instead the disc–field interaction adds a considerable amount of angular momentum to the inner disc, the disc density

structure and $r_{\rm m}$ will become 'trapped' close to $r_{\rm c}$, so that even as $\dot{M}$ decreases the disc will stay near $r_{\rm c}$ and accretion will continue (Sunyaev & Shakura 1977; D'Angelo & Spruit 2010, hereafter DS10; D'Angelo & Spruit 2012). As a result, the spin-down rate as a function of accretion rate will be significantly different from equation (3) or (4). For a normal accretion disc, this condition will at least be true for $r_{\rm m} < 1.3\,r_{\rm c}$, since the energy available through differential rotation between the field and disc is not enough to expel gas at a rate that matches the accretion rate in the disc. Depending on how efficiently gas can be loaded into an outflow, this situation can also apply for larger truncation radii.

However, once a trapped disc has formed, the inner edge of the disc is no longer given by an equation of the form equation (1). Instead, $r_{\rm m}$ is almost independent of $\dot{M}$ and is determined by balancing the torque from the disc–field interaction, $\tau_{\rm B}$, with torque transmitted outwards by viscous stress in the disc, so that:

$$3\pi\nu\Sigma(r_{\rm m})r^2\Omega_{\rm K}(r_{\rm m}) = \tau_{\rm B} = \eta r^2 \Delta r B^2, \qquad (6)$$

where $\nu$ and $\Sigma$ are, respectively, the effective viscosity and surface density of the accretion disc. In consequence, the accretion rate through the inner disc can decrease to a very low rate or even drop to zero, but the inner disc edge will never move very far from $r_{\rm c}$.

DS10 and D'Angelo & Spruit (2011, 2012) studied accretion disc behaviour in these conditions, and found that accretion proceeded either continuously or in short accretion bursts (much faster and weaker than full accretion outbursts). Depending on the strength of the coupling between the field and the disc, they also found that the star could be efficiently spun down by the presence of a disc, even when the accretion rate is extremely low. D'Angelo & Spruit (2012) called this state a 'trapped disc', because the inner disc edge remains trapped close to $r_{\rm c}$ as the average $\dot{M}$ through the outer disc decreases.
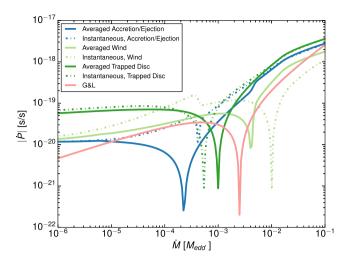
Spin regulation in the trapped disc model superficially resembles the model suggested by GL, since accretion on to the star continues even though the star is being spun down. However, it is fundamentally different, in that it incorporates a more physically realistic, potentially non-steady picture for the interaction between the disc and the magnetic field coupling region, rather than the steady-state, extended region of coupled field lines in GL. Rather than focus in detail on how the disc and the magnetic field couple (which simulations show is likely a complicated and non-steady process), DS10 instead assumed that the disc–field interaction adds angular momentum to the disc, and demonstrated how the disc structure changes as a result of this interaction. Furthermore, since the DS10 model has a self-consistent description for the disc as a function of accretion rate for all accretion rates, it does not breakdown at low $\dot{M}$ like the model of GL (which has no steady accretion solutions $r_{\rm m} > r_{\rm c}$).

The rotating magnetic field provides an additional spin-down torque (comparable to angular momentum loss from a rotating magnetic dipole in vacuum):

$$\dot{j} = -\frac{2\mu^2\Omega^3}{3c^2}. \qquad (7)$$

Except for weak-field accreting millisecond X-ray pulsars (AMXPs) at low $\dot{M}$, this is essentially negligible (but is included in all calculations for completeness).

The solid lines in Fig. 1 show the spin change induced in a weak-field NS as a function of accretion rate for the accretion/ejection model (dark blue), stellar wind (light green), and trapped disc (dark green). The spin change predicted by GL is also shown in pink for comparison. At high accretion rates all the solutions converge, adding angular momentum at a rate $\dot{M}(GMr_{\rm m})^{1/2}$. At low accretion



**Figure 1.** Expected spin change (absolute value) as a function of the average accretion rate for an accreting millisecond pulsar with the canonical parameters given in Table 1 for different spin regulation models. The solid curves trace the net spin change after an outburst cycle (shown in Fig. 2 and scaled to $\langle\dot{M}\rangle$). The dashed lines show the same spin change curves considering only the average accretion rate. (Note that $|\dot{P}|$ is plotted; there is a sign change at the singularity and at low $\dot{M}$ the star spins down.)

rates, the effect of the trapped disc becomes clear: unlike in the accretion/ejection picture or when there is a stellar wind, the trapped disc is able to keep spinning down the star efficiently.

## 3 METHOD SUMMARY

During an accretion outburst, the spin period derivative is expected to change with the accretion rate. Here, I want to investigate whether the net spin change across the whole accretion/quiescent cycle is the same as predicted from the cycle-averaged accretion rate. The method used to calculate the equilibrium spin period and time-scale for magnetic stars going through accretion outbursts is described in detail below. In brief, I first define an accretion outburst profile, $\dot{M}(t)$ with average accretion rate $\langle\dot{M}\rangle$, and calculate the time-dependent torque $\dot{J}(\dot{M}(t))$ for a given spin-down model, which is then averaged over the outburst to get $\langle\dot{J}(\dot{M}(t))\rangle$. In general, this can be very different from $\dot{J}(\langle\dot{M}\rangle)$, i.e. the torque from the time-averaged accretion rate. The solid and dot–dashed curves in Fig. 1 show how the net torque on a star changes with accretion rate, either considering the effect of accretion bursts (the solid lined 'average' curves) or not (the dot–dashed 'instantaneous' curves).

To calculate the spin evolution of a star, I then calculate a series of $\langle\dot{J}(\dot{M}(t), P_*)\rangle$, i.e. the angular momentum change as a function of accretion rate for a wide range of stellar spin periods (as shown in Fig. 3, where I have plotted the $\dot{P}$, the stellar spin period change rather than the analogous $\dot{J}$). I then use this series of curves to evolve the star's spin for a given average accretion rate until it converges to a fixed spin period.

The time it takes to converge is the spin-equilibrium time, $T_{\rm eq}$ and the final spin period at convergence is the spin-equilibrium period, $P_{\rm eq}$. $T_{\rm eq}$ and $P_{\rm eq}$ for different torque models and outburst properties can then be compared to analytic estimates without accounting for accretion bursts (i.e. considering $\dot{J}\langle\dot{M}\rangle$).

### 3.1 Note on units, conversions for different types of systems

Where possible, all results in this paper are given in terms of scale-invariant variables that can be applied to different

**Table 1.** Adopted canonical values for different types of astrophysical systems.

| Star | Mass $(M_\odot)$ | Radius (cm) | $B_*$ (G) | $I_*$ (g cm²) | $\langle \dot{M} \rangle$ $(M_\odot \text{ yr}^{-1})$ | $P_{\text{eq},0}$ | $T_{\text{eq},0}$ (yr) | $R_m/R_*$ | $R_c/R_*$ |
|---|---|---|---|---|---|---|---|---|---|
| Pulsar | 1.4 | $10^6$ | $10^{12}$ | $10^{45}$ | $1.4 \times 10^{-9}$ | 0.7 s | $2 \times 10^5$ | 130 | 170 |
| AMXP | 1.4 | $10^6$ | $10^8$ | $10^{45}$ | $1.4 \times 10^{-11}$ | 0.002 s | $6 \times 10^9$ | 2.5 | 2.7 |
| Intermediate polar | 0.6 | $10^9$ | $10^6$ | $10^{50}$ | $1.6 \times 10^{-10}$ | 1200 s | $2 \times 10^6$ | 14 | 13 |
| TTauri star | 0.5 | $1.4 \times 10^{11}$ | $2 \times 10^3$ | $4 \times 10^{54}$ | $5 \times 10^{-8}$ | 2 d | $3 \times 10^5$ | 2.7 | 3.4 |

magnetized accreting stars – NSs with high ($\sim 10^{12}$G) magnetic fields (X-ray pulsars) and low ($\sim 10^8$G) magnetic fields (AMXPs or non-pulsating NSs with low-mass companions), magnetic white dwarfs, and TTauri stars. Table 1 gives typical values of $B_*$, $P_*$, $\dot{M}$, $r_m$, etc. for different astronomical objects.

Each torque model has several numerical parameters that I explore in individual subsections. For the 'canonical' versions of each model, I adopt the following parameters:

(i) in all models, $\xi = 0.4$ (the numerical factor modifying equation (1) to set the location of $r_m$)

(ii) for the 'accretion/ejection' and 'wind' models, I adopt a smoothing length $\Delta r_2 / r = 0.1$, while the wind has an assumed outflow rate of $0.1\dot{M}$

(iii) in the 'trapped disc' model, $\Delta r / r = \Delta r_2 / r = 0.1$.

The results in Section 4 use the stellar parameters of a millisecond X-ray pulsar (AMXP) listed in Table 1. In Sections 5.1–5.3, I discuss in more detail the simulation results specific different types of magnetic star and implications for spin evolution in these systems.

## 3.2 Modelling the accretion outburst

I use a simple fast-rise/exponential-decay function to model an accretion outburst. This model has two free parameters: the duration of the outburst and the ratio between maximum and minimum accretion rate:
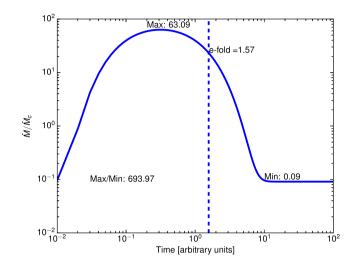
$$\dot{M}(t) = e^{\sqrt{2/F_t}} e^{-1/10t - 10t/F_t} + \dot{M}_{\text{min}}, \qquad (8)$$

where $\sim F_t/5$ is the decay time and $\dot{M}_{\text{min}}$ is the quiescent accretion level through the disc. The ratio between outburst maximum and quiescence is then:

$$\frac{\dot{M}_{\text{max}}}{\dot{M}_{\text{min}}} \simeq \frac{e^{-0.6/\sqrt{F_t}}}{\dot{M}_{\text{min}}} + 1. \qquad (9)$$

The outburst duration is arbitrarily set to 100, so that $F_t/5$ is a rough measure of the duration of the outburst (the rise times are assumed to happen extremely rapidly for simplicity). The light curve is then renormalized to 1 (which is why $\dot{M}_{\text{min}}$ does not always match the actual quiescent $\dot{M}$ in some figures).

The 'canonical' burst profile adopted in this paper is shown in Fig. 2. In this model $\dot{M}_{\text{min}} = 0.0014 \dot{M}_{\text{max}}$, $\dot{M}_{\text{min}} = 0.1$, and the outburst duration (defined as when the accretion rate is within $1/100e$ of maximum) is $F_t = 10$. In Section 4.1, I explore how changing the outburst duration and amplitude changes the spin period. I have also explored other outburst shapes to confirm that changing the functional form of the outburst (e.g. to a linear rise and decay function) makes only small quantitative changes in the results, provided there is a consistent outburst duration.



**Figure 2.** Accretion rate as a function of time, scaled to $\dot{M}_c$, the nominal equilibrium accretion rate for different spin periods. Accretion outbursts are modelled by a 'fast-rise, exponentially decaying' function above a quiescent accretion level, where the outburst duration and ratio of peak $\dot{M}$ to quiescent $\dot{M}$ are free parameters.

## 3.3 Calculating $\dot{J}$ for different stellar spin periods and $\dot{M}$

From the accretion profile $\dot{M}(t)$ and a given model for the instantaneous angular momentum exchange between disc and star (Sections 2.2–2.4), the net angular momentum exchange over an entire outburst is calculated for different average accretion rates. $\dot{J}(\dot{M})$ is a function of stellar spin as well as the current accretion rate. This can be made scale invariant by scaling the accretion rate by the 'critical' accretion rate:

$$\dot{M}_c = \xi r_c^{-7/2} \mu^2 (GM_*)^{-1/2}, \qquad (10)$$

i.e. the accretion rate at which $r_c = r_m$. Written this way, $\dot{J}$ can be written as a function of a single variable, $\dot{J}(\dot{M}/\dot{M}_c)$.

Additional physical effects break the scale invariance of $\dot{J}(\dot{M}/\dot{M}_c)$. At very low $\dot{M}$, spin-down can become dominated by magnetic dipole radiation for an AMXP. At high $\dot{M}$, NSs can reach the Eddington limit ($\dot{M}_{\text{Edd}} \simeq 8.7 \times 10^{17}$ g s$^{-1}$ for a $1.4 M_\odot$ NS), which I assume is the maximum accretion rate on to the stellar surface (thus limiting spin-up). Finally, in both TTauri stars and AMXPs at high $\dot{M}$, the accretion flow can crush the magnetosphere and fall directly on the star. In this case, the torque on the star can be very different (see e.g. Paczynski 1991; Popham & Narayan 1991). Since this is not the focus of this paper, I simply assume that when the calculated $r_m < R_*$, the angular momentum added to the star at a rate of $\dot{M}(GM_* r_*)^{1/2}$. I similarly do not put a limit at the breakup frequency for the stars, since at very high $\dot{M}$ where this is most relevant magnetospheric accretion will have ceased and it is not clear how angular momentum is regulated.
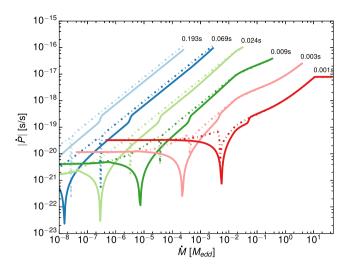
**Figure 3.** Spin change as a function of $\dot{M}$ for the accretion/ejection scenario. The different curves represent different stellar spin periods (labelled above each curve). The dashed lines show the expected spin-down profiles for $\dot{P}$ as a function of a given instantaneous accretion rate. The minimum occurs at the spin-equilibrium point, where the star switches from spin-up to spin-down. The solid curves instead plot $\langle \dot{P}(\dot{M}(t)) \rangle$, the change in the net $\dot{P}$ as a function of $\dot{M}$ integrated over the entire outburst (the solid curves). Considering an outburst can dramatically alter the spin change of the star, decreasing $\dot{P}$ considerably over a wide range of $\dot{M}$ and shifting the 'spin equilibrium' accretion rate systematically lower. The simple form of the function is broken by dipole spin-down at low $\dot{M}$, and the Eddington limit at high $\dot{M}$.

Fig. 3 shows the spin rate change, $\dot{P}(\dot{M})$ of the 'canonical' NS in response to the accretion/ejection torque model. In all figures I plot $\dot{P}$ versus $\dot{M}$ rather than $\dot{J}$ versus $\dot{M}$ to make the figures easier to relate to observations. The two quantities are related by:

$$\dot{P} = -\frac{\dot{J} P_*^2}{2\pi I_*}, \tag{11}$$

where $P_*$ is the stellar period and $I_*$ the star's moment of inertia. Each curve shows $\dot{P}(\dot{M})$ for a different spin period (ranging between $P_* = 0.001$–$0.2$ s). The dot–dashed lines show the spin change as a function of the average accretion rate ($\dot{P}(\langle \dot{M} \rangle)$; equation 3). The solid lines show $\langle \dot{P}(\dot{M}) \rangle$, the spin derivative averaged over the entire accretion outburst and quiescence (calculated using the outburst profile given in Fig. 2).

The singularity marks the 'spin-equilibrium' point, where the net torque on the star is zero and there is no spin change. At accretion rates less than equilibrium the star spins down, while for higher $\dot{M}$ it spins up. The spin-down at very low $\dot{M}$ is dominated by pulsar dipole radiation (relevant for AMXPs). At high accretion rates, the spin-up torque on the star levels off as the inner edge of the accretion disc first touches the star and then the outburst accretion rate reaches the Eddington limit.[1]

The differences between the dashed and solid sets of curves are clear. First $|\dot{P}|$ over an outburst is much smaller than the instan-

---

[1] Andersson et al. (2005) explicitly considered accretion from an Eddington-limited disc on to an NS, and found a different angular momentum exchange rate than the one presented here. This could be incorporated into this work, but is currently omitted for simplicity, and to make it easier to translate between different types of magnetic star.

---

taneous spin change for a large range of accretion rates close to equilibrium. This means the total torque on the star is considerably smaller than simple calculations would predict, which significantly increases the time the star takes to reach spin equilibrium ($T_{eq}$). The second effect is to shift the equilibrium accretion rate to a lower $\dot{M}$, which means that $P_{eq}$ is significantly faster than equation (3) would predict for a given average accretion rate.

Fig. 1 shows $\dot{P}(\langle \dot{M} \rangle)$ and $\langle \dot{P}(\dot{M}) \rangle$ for the different models of stellar angular momentum loss presented in Sections 2.2–2.4, using the 'canonical' model parameters introduced above. Again, solid curves show the net $\dot{P}$ averaged over an outburst, while the dashed curves show the instantaneous $\dot{P}$ for a given accretion rate. For comparison, the model of GL (as approximated by Ho et al. 2014) is overplotted in dark green.

The main difference between the accretion/ejection model (blue), wind (light green), and trapped disc model (dark green) is seen at low $\dot{M}$. In a trapped disc at low accretion rates, the torque from the disc/field interaction remains strong, whereas for the other two models spin-down is dominated by dipole radiation. The shape of the accretion/ejection and wind models are asymmetric around the equilibrium minimum. The minimum is also shifted relative to the curves showing the instantaneous $\dot{P}(\dot{M})$, corresponding to a different equilibrium spin period. In contrast, the trapped disc shows a much more modest change in shape, although the equilibrium $\dot{M}$ is also significantly shifted. These differences underscore the intrinsic model dependence in inferring properties of the star (like the B field) from the assumption of 'spin equilibrium' in a magnetic star.

### 3.4 Spinning the star towards equilibrium

Finally, I use the set of curves $\langle \dot{J}(\dot{M}, \dot{M}_c) \rangle$ calculated in the previous section to find $P_{eq}$ and $T_{eq}$ for a given angular momentum model. For a given average $\dot{M}$ and assumed stellar moment of inertia $I_*$, I evolve the spin rate of the star in time in response to the torque $\langle \dot{J}(\dot{M}, \dot{M}_c) \rangle$ using a fifth-order Runge–Kutta integration scheme implemented as 'dopri5' in the SCIPY library until the spin period converges.
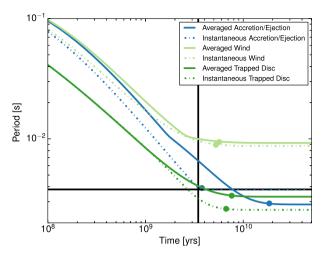
I define the spin-equilibrium time, $T_{eq}$, as the evolution time for the spin period from $(1 \pm \epsilon)P_0$ to $(1 \pm \epsilon)P_f$, where $\epsilon = 10^{-3}$ is an arbitrary parameter and $P_0$, $P_f$ are the initial and final spin periods). The $\pm$ sign is used appropriately depending on whether the star spins up or down as a result of accretion. The calculated spin-equilibrium period is then defined as the spin period at $T_{eq}$.

Fig. 4 shows the final stages of spin evolution for an AMXP accreting at $\dot{M}_0 = 2 \times 10^{-4} \dot{M}_{Edd}$. The different colours correspond to the different torque models (as in Fig. 1), for both $\langle \dot{P}(\dot{M}) \rangle$ (solid) and $\dot{P}(\langle \dot{M} \rangle)$ (dot–dashed). The closed circles indicate the numerically calculated $T_{eq}$ and $P_{eq}$ for each spin-down curve.
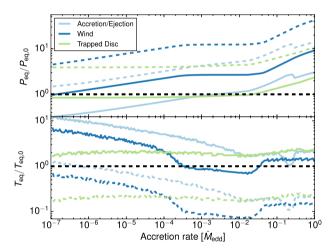
Vertical and horizontal lines mark the analytic predictions for the equilibrium spin period, $P_{eq, 0}$ calculated based on $\langle \dot{M} \rangle$:

$$P_{eq, 0} \sim \frac{2\pi}{\sqrt{GM_*}} r_m^{3/2}$$

$$P_{eq, 0} \simeq 3.2\,\mathrm{ms} \left( \frac{\xi}{0.4} \right)^{3/2} \left( \frac{M_*}{1.4 M_\odot} \right)^{-5/7}$$

$$\times \left( \frac{\mu}{10^{26}\,\mathrm{G\,cm^3}} \right)^{6/7} \left( \frac{\dot{M}}{2 \times 10^{-4} \dot{M}_{Edd}} \right)^{-3/7}, \tag{12}$$

**Figure 4.** The final spin evolution of the 'canonical' NS, for the same initial parameters but different torque models (accretion/ejection, wind, and trapped disc). The horizontal solid line marks the expected equilibrium spin period, $P_{eq}$ while the vertical line marks $T_{eq}$. The circles indicated the point $(T_{eq}, P_{eq})$ for each model.



**Figure 5.** $P_{eq}$ (top) and $T_{eq}$ (bottom) for each torque model, accounting for outbursts, divided by the $P_{eq}$ and $T_{eq}$ predicted by simple analytic estimates (see the text for details). The solid line compares the two quantities with the values obtained by taking $\langle \dot{M}_{tot} \rangle$ (i.e. the total-averaged accretion rate), while the dashed line estimates $T_{eq}$ and $P_{eq}$ considering only average accretion rate during outburst $\langle \dot{M} \rangle_{out}$.

and the characteristic spin-down time, $T_{eq,0} \simeq \dot{P}/P$:
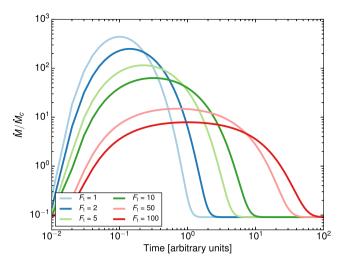
$$T_{eq,0} \sim \frac{2\pi I_*}{P_{eq}\dot{M}(GM_* r_m)^{1/2}}$$

$$T_{eq,0} \simeq 3.5 \times 10^9 \text{yr} \left(\frac{I_*}{10^{45}\text{g cm}^2}\right)\left(\frac{\xi}{0.4}\right)^{-2}\left(\frac{M_*}{1.4\,M_\odot}\right)^{2/7}$$

$$\times \left(\frac{\dot{M}}{2\times 10^{-4}\dot{M}_{Edd}}\right)^{-3/7}\left(\frac{\mu}{10^{26}\text{G cm}^3}\right)^{-8/7}. \qquad (13)$$

Both $P_{eq}$ and $T_{eq}$ can be substantially different from the values given by equations (12) and (13). $P_{eq}$ and $T_{eq}$ are sensitive to both the torque model used and the properties of the outbursts (their amplitude and duration), as well as the location of the inner disc edge, and the specific details of the torque model itself.

Fig. 5 shows $P_{eq}$ and $T_{eq}$ (calculated and illustrated in Fig. 4) as a function of $\dot{M}$. To emphasize the difference between simple



**Figure 6.** Outburst accretion profiles for different outburst duration, keeping the net accretion rate fixed (so that shorter outbursts have larger maxima). The outburst duration varies from 0.2 to 20 per cent of the accretion cycle.

estimates and more realistic calculations, both $P_{eq}$ and $T_{eq}$ here scaled by equations (12) and (13). The solid curves scale the results using the average $\dot{M}$, while the dashed curves show the results scaled to $T_{eq,0}$ and $P_{eq,0}$ calculated using the *outburst* accretion rate $\langle \dot{M} \rangle_{out}$, as is sometimes done in the literature (e.g. Klus et al. 2014).[2]

Neither $\langle \dot{M} \rangle$ nor $\langle \dot{M} \rangle_{out}$ gives a reliable measure of $T_{eq}$ and $P_{eq}$ at all accretion rates, with deviations of up to an order of magnitude in the estimated value. $P_{eq}$ and $T_{eq}$ tend to follow a power-law relationship with $\langle \dot{M} \rangle$ for low accretion rates, which is broken at higher accretion rates by $\dot{M}_{Edd}$. In particular, the conclusion that a stronger magnetic field leads to a slower star (equation 12) is significantly complicated by outbursts, and depends to some extent on the dominant angular momentum loss mechanism.

Additionally, $T_{eq}$ is considerably longer than expected, which could mean that spin equilibrium is unlikely. This is especially true for millisecond pulsars, where $T_{eq}$ can easily stretch to $10^9$ yr at $\sim 10^{-3}\dot{M}_{Edd}$, and TTauri stars, which have outburst cycles that could be a significant fraction of $T_{eq,0}$ (see section 5.3).
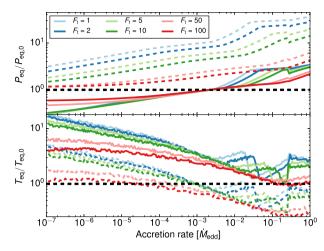
## 4 RESULTS
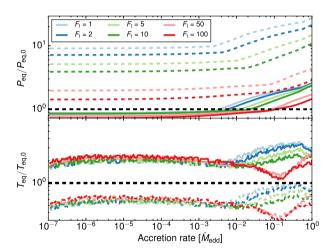
### 4.1 Changing outburst duration and amplitude

Accreting stars show a wide range of outbursting behaviour, with dramatic differences in outburst durations and amplitudes. Here, I investigate how this changes the spin evolution, first by varying the outburst duration, then by varying its amplitude. In all cases, the average accretion rate is kept constant.

Fig. 6 shows $\dot{M}(t)$ profiles for outbursts of different duration, corresponding to $F_t = [1, 2, 5, 10, 50, 100]$ (cf. equation 8), with outburst durations $T_{out} = [0.5, 0.9, 2, 4, 15, 26]$ and $\dot{M}_{max}/\dot{M}_{min} = [4800, 2700, 1300, 700, 160, 90]$. The resulting $P_{eq}$ and $T_{eq}$ curves for the accretion/ejection and trapped disc models are shown in Figs 7 and 8. (The wind model shows the same qualitative behaviour as the accretion/ejection model, except that $P_{eq}$ is in general 2–3× longer, and $T_{eq}$ is typically within 50 per cent of $T_{eq,0}$, as in Fig. 5.)

---

[2] In this case, the predicted $T_{eq}$ will be increased by $1/f$, where $f$ is the fraction of time spent in outburst.
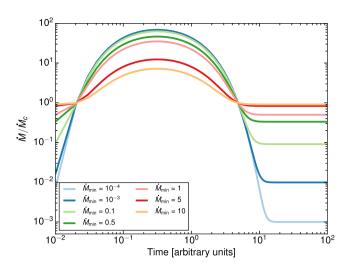
**Figure 7.** Effect of changing the outburst duration for the accretion/ejection model. For plot details see Fig. 5. As can be seen from the figure, neither $\langle \dot{M} \rangle_{\text{out}}$ nor $\langle \dot{M} \rangle$ can be used to give accurate estimates for $P_{\text{eq}}$ or $T_{\text{eq}}$, particularly for short outbursts (small $F_{\text{t}}$). The spin-equilibrium times are generically much longer than would be expected and the actual final spin periods are either considerably shorter (considering $\langle \dot{M} \rangle$) or longer ($\langle \dot{M} \rangle_{\text{out}}$) than expected. The results are similar for the wind model.



**Figure 8.** Same as Fig. 7 but for trapped disc model, in which spin-down continues during quiescence. The $T_{\text{eq}}$ is best predicted from the outburst accretion rate, although the final spin period is mainly determined by $\langle \dot{M} \rangle$.

The differences between the two models are clear. In the accretion/ejection model, $T_{\text{eq}}$ is sensitive to the outburst duration and neither $\langle \dot{M} \rangle_{\text{out}}$ nor $\langle \dot{M} \rangle$ give a reliable analytic estimate of $T_{\text{eq}}$ and $P_{\text{eq}}$. Moreover, the difference between estimating $P_{\text{eq}}$ from $\langle \dot{M} \rangle_{\text{out}}$ versus $\langle \dot{M} \rangle$ is largest for very short outbursts. For mean accretion rates above $\sim 10^{-4} \dot{M}_{\text{Edd}}$, $\langle \dot{M} \rangle$ gives a fairly reliable estimate for $P_{\text{eq}}$, while using $\langle \dot{M} \rangle_{\text{out}}$ predicts spin periods $P_{\text{eq}} \sim 10 \times$ shorter than the spin period from considering outbursts. However, using $\langle \dot{M} \rangle_{\text{out}}$ (corrected for the time spent in outburst) generally gives a more reliable estimate for $T_{\text{eq}}$ than $\langle \dot{M} \rangle$.

Interestingly, $P_{\text{eq}}$ increases above $P_{\text{eq, 0}}$ for very high accretion rates. Although this effect is modest, it only requires that accretion is Eddington-limited, not that spin-up efficiency is reduced (Andersson et al. 2005). Both effects together may significantly limit the maximum pulsar frequency without the need for other physical processes, such as gravitational wave emission (e.g. Bildsten 1998; Chakrabarty et al. 2003; Patruno, Haskell & D'Angelo 2012).



**Figure 9.** Outburst accretion profiles changing the mean quiescent level of accretion from $10^{-4}$ to 10, keeping the outburst duration the same. Since the accretion profile is normalized so that $\langle \dot{M} \rangle = 1$, $\dot{M}_{\text{max}}/\dot{M}_{\text{min}} = [7 \times 10^4, 7000, 700, 70, 15, 8]$ as the quiescent $\dot{M}$ increases.
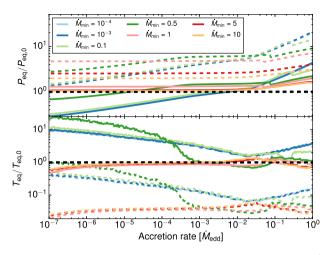
The trapped disc model in contrast is able to spin-down the star at very low $\dot{M}$ so $P_{\text{eq}}$ and $T_{\text{eq}}$ are fairly insensitive to changes in $\langle \dot{M} \rangle$. Using $\langle \dot{M} \rangle$ in equations (12) and (13) thus gives the best estimate for $P_{\text{eq}}$ and $T_{\text{eq}}$; $P_{\text{eq}} \sim 0.8 P_{\text{eq, 0}}$, while $T_{\text{eq}}$ is about twice as long. As $\langle \dot{M} \rangle$ increases the spin period becomes longer than predicted, because the accretion rate (and hence spin-up) becomes Eddington-limited. $T_{\text{eq}}$ increases relative to $T_{\text{eq, 0}}$, although again by a modest factor. In summary, the trapped disc model matches well with analytical predictions provided $\langle \dot{M} \rangle$ is used rather than $\langle \dot{M} \rangle_{\text{out}}$.

There is a wide variation in outburst durations in accreting stars. Observed duty cycles for outbursting Be X-ray binaries are typically 5–20 per cent (Reig 2011; Klus et al. 2014, see also Section 5.2), while for AMXPs the rate is more likely 2–3 per cent (Yan & Yu 2015), and for TTauri stars is essentially unknown (Hillenbrand & Findeisen 2015 assume $\sim 1$ per cent).
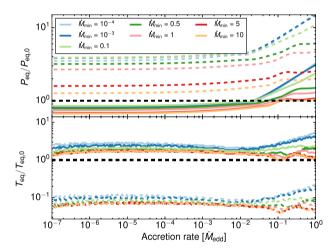
The amplitude of the outbursts can also significantly affect the spin evolution. Fig. 9 shows $\dot{M}(t)$ for a constant outburst duration but amplitude variations over five orders of magnitude, $\dot{M}_{\text{max}}/\dot{M}_{\text{min}} = [7, 15, 70, 150, 700, 7000, 7 \times 10^4]$. Observed outburst amplitudes vary from $\sim 10$ to 1000 (Be X-ray binaries; Reig 2011), $\sim 10^3$ (TTauri stars, assuming they all undergo FU Ori-type outbursts; Hillenbrand & Findeisen 2015; Section 5.2) and $10^4$–$10^5$ (AMXPs).

$P_{\text{eq}}$ and $T_{\text{eq}}$ for the accretion/ejection model are shown in Fig. 10. Both of these values show somewhat complicated behaviour at different $\dot{M}$ and for different outburst amplitudes. Predictably, for smaller outburst amplitudes $P_{\text{eq}}$ and $T_{\text{eq}}$ stay very close to $P_{\text{eq, 0}}$ and $T_{\text{eq, 0}}$. For larger contrasts ($\dot{M}_{\text{max}}/\dot{M}_{\text{min}} > 100$), the equilibrium spin periods are much shorter than would be predicted from $\langle \dot{M} \rangle$, but are also generally significantly longer than predicted by $\langle \dot{M} \rangle_{\text{out}}$. Likewise, $T_{\text{eq}}$ is not well predicted from either $\langle \dot{M} \rangle$ or $\langle \dot{M} \rangle_{\text{out}}$. As the accretion rates become Eddington-limited (which happens at progressively lower $\langle \dot{M} \rangle$ for increasing outburst amplitude), $P_{\text{eq}}$ and $T_{\text{eq}}$ in all cases start to more closely match predictions. These results again emphasize the limitations of inferring quantities like the stellar magnetic field from assumptions of spin equilibrium and steady accretion.

Similar to changing the outburst duration, changing the outburst amplitude has a minimal effect on $P_{\text{eq}}$ and $T_{\text{eq}}$ in the trapped disc scenario (Fig. 11). There is a modest increase in $P_{\text{eq}}$ and $T_{\text{eq}}$ for

**Figure 10.** Same as Fig. 5, but now changing the outburst amplitude $\dot{M}$, using the accretion/ejection torque model. The different colours correspond to the outbursts with different total amplitudes (Fig. 9). As for the cases shown in Figs 7 and 8, the $T_{eq}$ is reasonably well predicted by the outburst $\dot{M}$, while the $P_{eq}$ is better predicted from $\langle \dot{M} \rangle$.
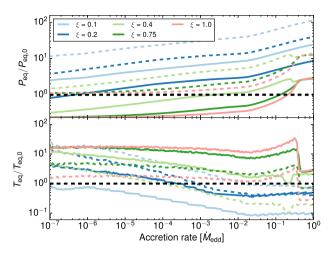


**Figure 12.** Effects of changing inner radius of the disc ($\xi$) on the accretion/ejection model. The plot shows the $P_{eq}$ (top) and $T_{eq}$ (bottom) as a function of $\langle \dot{M} \rangle$ for different $\xi$ values, analogous to Fig. 5.



**Figure 11.** Same as Fig. 5, but now changing the outburst amplitude $\dot{M}$, using the trapped disc model. The different colours correspond to the outbursts with different total amplitudes (Fig. 9).
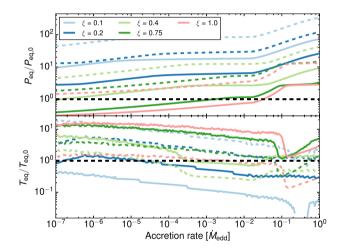


**Figure 13.** Effects of changing inner radius of the disc ($\xi$) on the wind model. The plot shows the $P_{eq}$ (top) and $T_{eq}$ (bottom) as a function of $\langle \dot{M} \rangle$ for different $\xi$ values, analogous to Fig. 5.

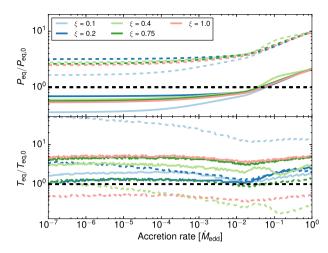larger outburst amplitudes, which is the same for all $\langle \dot{M} \rangle$ except at the highest accretion rates.

## 4.2 The effect of changing $r_m$ ($\xi$) on spin evolution

As discussed in Section 2.1, the location of the inner edge of the disrupted disc could depend on the structure of the accretion flow, magnetic field configuration, and efficiency of coupling between the disc and the field. The location of $r_m$ also determines $\dot{M}_c$, the 'critical' accretion rate that marks the transition from predominantly spin-up to spin-down. All these effects can lead to changes in the spin-down efficiency. Here, the uncertainty in $r_m$ is parametrized by $\xi$ in equation (1), which is usually assumed to lie between $\xi \sim 0.4$ and 1 (Frank, King & Raine 2002). In this paper, I explore a larger range for $\xi \sim 0.1$–1. This is motivated in part by the fact that changing $\xi$ changes $\dot{M}_c$, so that there can be a considerable amount of spin-down at high accretion rates. This is motivated by the results of Zanni & Ferreira (2013) and others, who find significant outflows and angular momentum loss even at large accretion rates, which

means that the equilibrium accretion rate will be significantly larger than expected.

Although the location of $r_m$ is only uncertain by a factor of a few, the strong dependence of $\dot{M}$ on $r_m$ means that the *accretion rate* for which $r_m = r_c$ can be uncertain by a factor $\xi^{-7/2} = 300$ and $P_{eq} \propto \xi^{-3/2} \dot{M}^{-3/7}$ can lead to a 30-fold difference in spin period.

The results of this section demonstrate how different $\xi$ affect the long-term spin evolution of an outbursting star for the three different torque models, using the canonical outburst and stellar parameters introduced in Section 2. Figs 12–14 show $P_{eq}(\dot{M})$ and $T_{eq}(\dot{M})$ for the accretion/ejection, wind, and trapped disc models, with results scaled by equations (12) and (13) setting $\xi = 0.4$.

Figs 12 and 13 show the results for the accretion/ejection and wind models. In both models, $P_{eq}$ increases roughly linearly for decreasing $\xi$, while $T_{eq}$ is roughly proportional to $\xi$. The smaller $\xi$, the smaller $r_m$ for a given $\dot{M}$. Since $\dot{P} \propto \dot{M} r_m^{1/2}$, for small $\xi$ less angular momentum is added, limiting spin-up. Even neglecting $\xi < 0.4$, $P_{eq}$ and $T_{eq}$ are uncertain by $\sim 8 \times$ with the largest deviations at high $\dot{M}$. The uncertainty in $\xi$ also introduces uncertainty in whether using $\langle \dot{M} \rangle$ or $\langle \dot{M} \rangle_{out}$ will more accurately predict $P_{eq}$, which again

**Figure 14.** Effects of changing inner radius of the disc ($\xi$) on the trapped disc model. The plot shows the $P_{eq}$ (top) and $T_{eq}$ (bottom) as a function of $\langle \dot{M} \rangle$ for different $\xi$ values, analogous to Fig. 5.

underscores the difficulty in constraining physical parameters from assumptions of spin equilibrium.

In the trapped disc picture (Fig. 14), $T_{eq}$ shows a much weaker dependence on $\xi$ and $P_{eq}$ is nearly independent of it. This is because $r_m$ in a trapped disc always stays close to the corotation radius and continues to extract angular momentum efficiently for all $\xi$. In general, however, $T_{eq}$ is longer by $\sim 2$–$5 \times$ than would be expected from analytic estimates, again raising the question about whether spin equilibrium is a good assumption, particularly for systems (like protostars or AMXPs) in which the total duration of accretion could be comparable to $T_{eq}$. This is discussed further in Sections 5.1–5.3.

### 4.3 Exploring uncertainties in the 'accretion/ejection' scenario

The simplest 'accretion/ejection' picture for magnetospheric accretion is one in which gas is accreted at high $\dot{M}$, expelled in a centrifugally launched 'propeller' outflow at low $\dot{M}$, and shows both infall and outflow for a range of intermediate $\dot{M}$. This model is approximated by equation (3). Numerical MHD simulations generically indicate that the disc–field interaction is time-dependent, and show some accretion and outflow for all $\dot{M}$. As a result there can be significant angular momentum loss while the star is actively accreting (as observed by Zanni & Ferreira 2013), and some residual accretion reaches the star even in the strong 'propeller' regime, but how much or how the accretion/outflow efficiency with $\langle \dot{M} \rangle$ is unclear. D'Angelo et al. (2015) used numerical simulation results to quantify the ejection efficiency (fraction of gas expelled in an outflow) as a function of accretion rate, which suggest propeller efficiencies of up to $\sim 95$ per cent in the strongest propeller simulations. In equation (3), the transition from 'propeller' to 'accretion' is parametrized by $\Delta r_2$, which gives the range of $r_m$ which have both accretion and ejection (or equivalently, the range of $\langle \dot{M} \rangle$ where this is the case, $\Delta \dot{M} \equiv -7/2 \Delta r_2 / r \dot{M}$).

Fig. 15 shows how the star's spin rate changes with $\dot{M}$ for different values of $\Delta r_2$ in the 'accretion/ejection' torque model. To emphasize how little $\Delta r_2$ affects $\dot{P}$, the figure shows $\dot{P}(\dot{M})$ for $\Delta r_2$ across four orders of magnitude: $\Delta r_2 / r = 10^{-2..2}$. As in previous figures, the solid lines show the outburst-averaged $\dot{P}$, $\langle \dot{P}(\dot{M}) \rangle$, while the dot–dashed lines show the 'instantaneous' spin rate change, $\dot{P}(\langle \dot{M} \rangle)$.

As the figure shows, $\Delta r_2$ has a very strong effect on the instantaneous torque on the star, generally suppressing both spin-up and
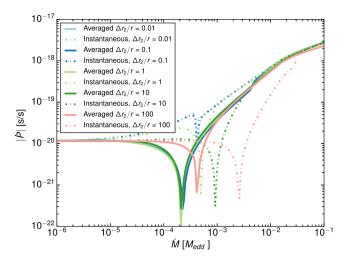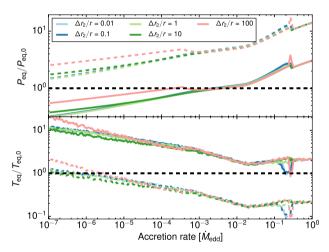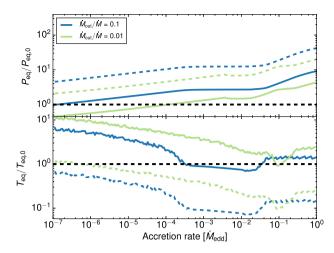


**Figure 15.** The spin-down rate as a function of accretion rate in the accretion/ejection model, for a star with $P_* = 0.003$ s. The different dashed curves show the effect of changing the smoothing parameter $\Delta r_2 / r$ in equation (3). This changes the range of $\dot{M}$ in which the inner disc is close to $r_c$ and there is simultaneously spin-up and spin-down, before moving to a 'true' ejection/accretion state. The solid lines show the torque averaged over an outburst, demonstrating that except for the very largest values of $\Delta r_2 / r$, the net torque is barely affected by the width of the transition region between propeller and accretion.



**Figure 16.** $P_{eq}$ and $T_{eq}$ curves corresponding to the different curves in Fig. 15. As is clear from the figure, the transition width between the propeller and accretion regimes makes very little difference in determining the final spin period or spin-equilibrium time.

spin-down efficiency and increasing $\dot{M}_c$ (the equilibrium accretion rate) as $\Delta r_2$ increases. However, the effect of increasing $\Delta r_2$ on the *outburst averaged* (and therefore long term) torque is minimal. As a result, $P_{eq}$ and $T_{eq}$ are essentially unaffected by changes in $\Delta r_2$, as shown in Fig. 16 because the accretion rate in outburst declines so rapidly that spin-down is only efficient (e.g. $\sim 3 \times 10^{-4}$ for $\Delta r_2 / r = 0.01$) for a short time.

This result indicates that even though the 'accretion/ejection' model adopted here is quite simplified, the detailed form of $\dot{J}(\dot{M})$ does not strongly influence the long-term evolution of an outbursting magnetic star.

**Figure 17.** Same as Fig. 5 for two different outflow rates from a stellar wind. When the outflow rate is high ($\sim 0.1 \dot{M}$) $P_{eq}$ becomes significantly slower than predicted, by a factor of $\sim 2$–10, depending on the accretion rate. A more significant effect is to decrease $T_{eq}$ to $\sim T_{eq, 0}$ across a wide range of accretion rate.
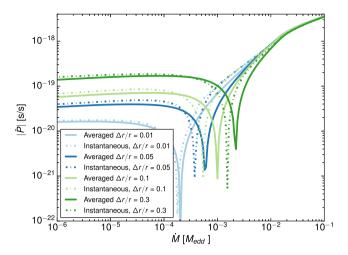
## 4.4 Changing the wind amplitude

In general, the conclusions of the previous section also apply to the accretion wind model (and explains why the results of this model are generally similar to the accretion/ejection one). In both cases, spin-down is inefficient when outbursts are considered because the accretion rate drops too quickly for the star to spend much time in the spinning-down phase.

Fig. 17 shows $P_{eq}$ and $T_{eq}$ for a strong ($\dot{M}_{out} = 0.1\dot{M}$) and weak ($\dot{M}_{out} = 0.1\dot{M}$) wind. For small outflow rates ($\sim 0.01\dot{M}$), the qualitative behaviour is essentially the same as for the accretion/ejection model, which indicates a stellar wind must be very strong (and requires a significant amount of accretion energy for launching) in order to significantly affect the spin evolution of the star. As long as $\dot{M}_{out}$ remains a free model parameter, it is difficult to say whether a stellar wind model is really a viable source for angular momentum loss. However, high-field NSs (which have the largest magnetospheres of any magnetically accreting star) show no indications of strong outflows, either as a radio source or through interaction with their environments, which might be expected for $\langle \dot{M}_{out} \rangle \sim 0.01$–$0.1\dot{M}_{Edd}$.
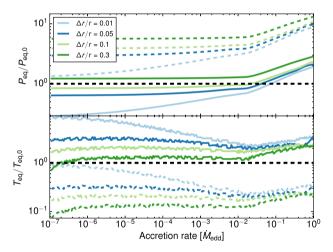
## 4.5 Exploring the trapped disc model

The trapped disc model also has two numerical parameters introduced in DS10, which mainly reflect our ignorance of the details of the disc–field interaction. The first is $\Delta r/r$, the width of the coupled region between the disc and the magnetic field (which sets the spin-down efficiency of the interaction). The second is $\Delta r_2/r$, which gives the range of $r_m$ over which there is both spin-up and spin-down (the same as in Section 4.3).

Figs 18 and 19 show how changing $\Delta r$ (i.e. the strength of the disc–field coupling) affects $\dot{P}$ and the overall spin evolution of a star. Fig. 18 shows $\dot{P}(\dot{M})$ curves for the canonical trapped disc parameters with increasing coupling strengths, $\Delta r = [0.01, 0.05, 0.1, 0.3]$. Increasing $\Delta r$ by 10 × increases $\dot{M}_{eq}$ by $\sim 5$, since a higher $\Delta r$ increases the spin-down efficiency, so that $P_{eq}$ is slower for the same $\langle \dot{M} \rangle$. There is a difference up to a factor 2 between the instantaneous and averaged $\dot{M}_{eq}$. For the canonical outburst profile, the disc is generally *more* efficient at spinning down the star than



**Figure 18.** Spin-down rate for the canonical stellar parameters for the trapped disc model, where different coupling strengths are assumed (corresponding to the width of the coupled disc–field region, $\Delta r/r$). Unlike the accretion/ejection picture, spin regulation continues in quiescence, so that there is only modest difference between using the actual outburst profile and the time-averaged one.
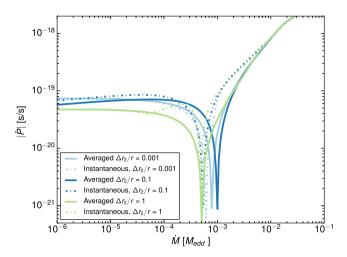


**Figure 19.** The ratio of $P_{eq}$ and $T_{eq}$ compared with the analytic prediction for a trapped disc with different coupling strengths (as shown in Fig. 18). The $T_{eq}$ is not significantly affected by the change of coupling strength, but the equilibrium period increases for increasing coupling strength (since spin-down is more efficient).
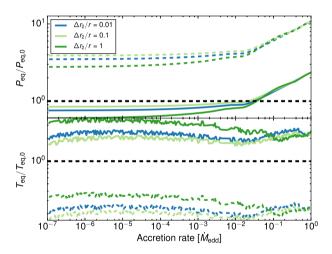
would be estimated from the naïve formula balancing spin-up and spin-down.

Fig. 19 shows $P_{eq}$ and $T_{eq}$ as a function of $\langle \dot{M} \rangle$ for the torque models plotted in Fig. 18. Since the star can only spin-down via interactions with the disc, if $\Delta r$ is very small $T_{eq}$ will be longer and $P_{eq}$ much shorter than expected (with increasing accuracy as $\langle \dot{M} \rangle$ increases). This effect is strongest for low accretion rates, where the spin-down torques dominate. As the mean accretion rate increases (and the magnetosphere becomes less important since the disc reaches the star), the differences between strong and weak spin-down decrease considerably. Finally, the figure shows (as is seen throughout this paper), that for a trapped disc $\langle \dot{M} \rangle$ is a better predictor for $T_{eq}$ and $P_{eq}$ than $\langle \dot{M} \rangle_{out}$.

Fig. 20 shows that increasing $\Delta r_2$ broadens the region around $\dot{M}_{eq}$ where the instantaneous torque is reduced. The effect on the outburst-averaged $\dot{P}$ is somewhat more subtle. For $\Delta r_2 = 0.1r$, $\dot{M}_{eq}$

**Figure 20.** Spin-down rate for the canonical stellar parameters for the trapped disc model, for different values of softening length $\Delta r_2/r$ (analogous to Figs 9–16). As in the accretion/ejection scenario, changing the softening length has a modest effect on the net torque on the star.



**Figure 21.** $P_{eq}$ and $T_{eq}$ for the system in Fig. 20. Changing the softening length has only a modest effect on the spin period and little influence on the $T_{eq}$.

is *higher* than for both $\Delta r_2 = r$ and $0.01r$, most likely related to the effects of accretion at large $\dot{M}$. This effect is modest (a factor of about two in $\dot{M}$) and might considerably change with the assumed outburst profile, so I do not explore it further.

The effects of changing $\Delta r_2$ on $P_{eq}$ and $T_{eq}$ are seen in Fig. 21. Here, again the differences between models are very modest and are close to the 'expected' values; $T_{eq}$ varies by $\sim 2 \times$ and $P_{eq} \lesssim 1.5 P_{eq, 0}$.

The conclusion of this and the previous section is that, compared with the differences between torque models and the uncertainties in accretion outburst details, the uncertainties in the individual torque models have a modest effect on the spin-equilibrium period or spin-down/up time-scale for the star. As long as there is efficient spin-down at some point, the different values of $\Delta r_2$ (total magnitude of the torque when $P_*$ is close to $P_{eq}$) does not matter. The most important difference remains what happens during quiescence – whether there is substantial spin-down (as in the trapped disc model) or not (the accretion/ejection and wind models).

## 5 DISCUSSION

This paper compares the long-term spin evolution of magnetized stars using different models for angular momentum regulation, explicitly considering the effects of time-variable accretion. Here, I briefly discuss the consequences of the results presented in Section 4 for three (very different) types of magnetically accreting, outbursting stars: TTauri stars, AMXPs, and Be/X-ray binaries. I focus on two questions in particular:

(i) Can observations be used to distinguish between the trapped disc pictures and other models for spin regulation?

(ii) How does considering a variable accretion rate alter predictions of the observable properties of strongly magnetized accreting stars?

### 5.1 Accreting millisecond X-ray pulsars and LMXBs

Accreting NSs with low magnetic fields ($\lesssim 10^8$ G) and low-mass companions (LMXBs) are thought to be the progenitors of radio millisecond pulsars (e.g. Alpar et al. 1982), spun up to millisecond spin periods via accretion over hundreds of millions of years. AMXPs are a subset of this group that show coherent pulsations and accretion outbursts, with peak luminosities reaching $\sim 20$ per cent $L_{\text{Edd}}$ (although most remain much fainter).

A second, partially overlapping subset of LMXBs have spin periods measured through quasi-periodic oscillations ('burst oscillations'), which are produced by localized, accretion-induced nuclear burning on the star's surface modulated by the star's rotation. These are an additional useful sample since the accretion rates in burst oscillation sources can be significantly larger than AMXPs. The spin periods inferred from burst oscillations are shorter on average than in than AMXPs (although the sample size remains small; Papitto et al. 2014). No periodicity has been detected in all remaining LMXBs, despite some very deep searches (Messenger & Patruno 2015), which could mean that the magnetic field in these sources is not strong enough to channel the accretion flow, at least during the brightest phases of the outburst.

What limits the spin frequency of the millisecond pulsars? Despite having relatively weak fields ($\sim 10^8$G; inferred from dipole spin-down) and long accretion times (the donor star lifetime is often $> 1$ Gyr), the fastest radio millisecond pulsar has a spin period of 1.4 ms (Hessels et al. 2006), much longer than the theoretical mass-shedding limit of $\sim 0.7$ms. Two possible mechanisms have been proposed – gravitational wave emission from a spin-induced quadrupole moment or $r$-modes (Bildsten 1998; Andersson, Kokkotas & Stergioulas 1999), or the spin-down effects from the magnetic field/disc interactions (e.g. Patruno et al. 2012), but it has proven difficult to definitively distinguish between them.

The spin distribution of radio millisecond pulsars peaks at a significantly longer spin period than that of AMXPs. Tauris (2012) has recently suggested that the difference in spin between the two populations could be significantly affected by the evolution of the mass-transferring companion. In this picture, AMXPs undergo a strong spin-down during the 'Roche lobe decoupling phase' as companion stops filling its Roche lobe so that the mass transfer rate to the pulsar decreases. Tauris (2012) estimated roughly 50 per cent of the pulsar's angular momentum can be lost during this phase, during which the average accretion rate drops by $\sim 3$ orders of magnitude.

The present work challenges the assertion that a decrease in $\dot{M}$ will efficiently spin the star down particularly if the accretion/ejection torque picture is the most relevant one. The results of Section 4 demonstrate the uncertainty in estimating $P_{eq}$ and $T_{eq}$:

between uncertainties in the star–disc interactions (e.g. the parameter $\xi$), the angular momentum loss mechanism, and the presence of accretion outbursts, $P_{eq}$ and $T_{eq}$ can both easily be uncertain by $10\times$, even when the physical parameters of the system ($\dot{M}$, $P_*$, $B_*$, $\dot{P}$) are well constrained. $T_{eq}$ lengthens with declining $\dot{M}$, so that as $\dot{M}$ decreases it takes progressively longer for the star to reach a new spin equilibrium. The results in this paper show that once outbursts are considered, $T_{eq}$ increases up to $10\times$.

Observations of AMXPs suggest that *none* of them are in spin equilibrium with their time-averaged accretion rates (considering both quiescence and outburst). On the other hand, systems with well-constrained spin derivatives show much less spin-up during outburst than might be expected from their luminosity Patruno & Watts (2012), which could indicate spin equilibrium. Watts et al. (2008) find the average luminosity (including quiescence) in AMXPs varies between $6 \times 10^{-5}$ and $0.02 L_{Edd}$ which implies (assuming radiative efficiency and the average NS parameters adopted in this paper) $P_{eq} \sim 1$–11 ms. AMXPs have observed spin periods between 1.7 and 5.5 ms, with no obvious trend as a function of mean luminosity (although some luminosities are uncertain by up to $10\times$ from distance and bolometric uncertainties). In particular, the recently discovered 'transitional pulsars' (Archibald et al. 2009; Papitto et al. 2013; Bassa et al. 2014), which switch between states of active accretion and radio pulsations, all have relatively fast spin periods (1.7–3.9 ms), despite extremely low accretion rates during outbursts for two of the three systems. For one of these sources, PSR J1023+0038, recent analysis of the X-ray pulsations has found spin-down during outburst is moderately larger than dipolar spin-down Jaodand et al. (2016) measured when the accretion disc is absent in the radio-loud phase.

None the less, radio millisecond pulsars (RMSPs) are observed to spin (on average) significantly slower than AMXPs, which would be possible even if a trapped disc remains present to spin-down the star even at very low $\dot{M}$. The spin-down in this case could happen gradually over the entire long-term decay phase of $\dot{M}$, rather than mainly being focused at early times in the 'Roche lobe decoupling phase', as suggested by Tauris (2012).

If the final large decline in $\dot{M}$ is not able to significantly spin down most pulsars in their late accretion phase, the question of what sets their maximum spin rate again becomes more urgent. In this paper, the 'canonical' $P_{eq}$ for an AMXP is about 0.4 ms at $\dot{M}_{Edd}$, but all simulations with outbursting accretion show slower rotation rates, typically by $\sim$1.5–3 $\times$ but up to $10\times$ in some cases. On the other hand, $T_{eq}$ at $\dot{M}_{Edd}$ is around 50 Myr (and increases when outbursts are considered). This is much shorter than the lifetimes of these systems, and (based on the observed sample of LMXBs) is unlikely to dominate the lifetime accretion rate of the star. As long as the star has a $\sim 10^8$G field, a lifetime average $\dot{M} \sim 0.1$–$0.01\dot{M}_{Edd}$ can limit the final spin period to within observed values without invoking an additional spin-down source like gravitational waves. (This is before considering modifications to the spin-up rate, e.g. Andersson et al. 2005, which may limit angular momentum transfer at high $\dot{M}$).

## 5.2 Be/X-ray Binaries

In strongly magnetized accreting NSs ($B \sim 10^{12}$G), dipole radiation is unimportant for spin regulation compared with spin change from accretion, and the spin rate of the star is determined by the interaction between the magnetic field and the accretion flow. The observed spin distribution ($P_* \sim 1$–1000 s) of these systems is much larger than in AMXPs, and many systems are observed to spin-up or down considerably. However, many accreting high-field NSs have

high-mass ($M > 3 M_\odot$) companions and are believed to mainly accrete from a wind rather than a disc (e.g. Bildsten et al. 1997), which is thought to give a much larger spread in $P_*$ and $\dot{P}_*$ than results from disc accretion.

A possible exception to this are Be/X-ray binaries, in which the NS undergoes accretion outbursts when it passes through the decretion disc of a companion Be star. Based on angular momentum conservation arguments, Klus et al. (2014) argue that as the pulsar passes through the Be star's disc most of the gas entering the pulsar's sphere of influence will have too much angular momentum to fall on to the star directly, implying that an accretion disc should form around the NS.

The *XMM–Newton* survey of the Small Magellanic Cloud (SMC) has tracked pulsars in Be X-ray binaries in the SMC over the past 14 yr, providing a unique data set to test spin evolution models (Coe et al. 2010). Ho et al. (2014) and Klus et al. (2014) argue that the small observed spin period derivatives suggest spin equilibrium (or else extremely low magnetic fields), and, if spin equilibrium is assumed, a surprisingly large fraction of Be X-ray binaries in the SMC should have magnetar-strength magnetic fields ($\sim 10^{14}$G). This is in contrast to systems in our own Galaxy with similar spin rates and luminosities, which have magnetic field estimates from cyclotron resonance emission lines on the order $B \sim 10^{12}$G.
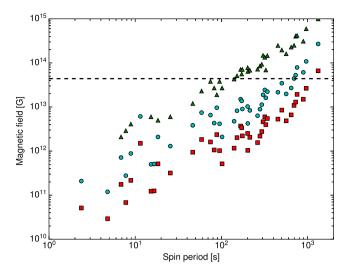
The conclusions of this paper suggest a somewhat different interpretation of the observations discussed by Klus et al. (2014), which reduce (although do not completely eliminate) the need for a very large magnetic field in most pulsars. Be X-ray binaries are generally transient, so that their average luminosity is much lower (typically several orders of magnitude) than their luminosity in outburst. To estimate the magnetic field, Klus et al. (2014) assume that the star is in spin equilibrium *with the outburst accretion rate* (see equation 12). This can be reasonable assumption if the accretion/ejection model applies, since in quiescence the torque on the star is strongly reduced. However, if a trapped disc remains present during quiescence, the star continues to spin-down, and it is more accurate to consider the *average* $\dot{M}$ rather than the outburst $\dot{M}$. (In fact, *Fermi* observations of some Be-X-ray binary systems indeed show that they spin-down between outbursts, see e.g. Sugizaki et al. 2015.)

To see how the results of this paper could affect estimates of $B_*$ in these systems, I calculate $P_{eq}$ (equation 12) assuming that spin equilibrium has been reached, using $\langle \dot{M} \rangle$ rather than $\langle \dot{M} \rangle_{out}$ (as was assumed by Klus et al. 2014). A rough estimate of $\langle \dot{M} \rangle$ for the stars in Klus et al. (2014) is given by:

$$\langle \dot{M} \rangle \simeq \dot{M}_{out} F_{out}, \tag{14}$$

where $\dot{M}_{out} \simeq 0.01$–$0.2\dot{M}_{Edd}$ (the inferred accretion rate from the outburst luminosity), and $F_{out} \simeq N_{det}/N_{obs}$ is the fraction of time spent in outburst (the ratio between the number of detections to observations). Klus et al. (2014) report 1–2 weekly observations (I use 84 observations/yr) over a timespan ranging from 0.15 to 14 yr, which corresponds to $F_{out} \simeq 0.004$–1 ($\langle F_{out} \rangle \sim 0.06$) and $\langle \dot{M} \rangle \simeq 7.5 \times 10^{-5}$–$0.2\,\dot{M}_{Edd}$. This assumes that the quiescent luminosity of these sources is at least $100\times$ lower than in outburst, which seems roughly consistent with observations (Coe, private communication).

Using equation (12), the estimated $\langle \dot{M} \rangle$, and the reported period for each pulsar from Klus et al. (2014), I estimate a revised magnetic strength, using either the accretion/ejection or trapped disc model. For simplicity, I choose the 'canonical' accretion/ejection and trapped disc models from Section 3.4, scaled to Be X-ray binary

**Figure 22.** Estimated magnetic field as a function of the spin period of Be X-ray binaries in the SMC. The green triangles show the values calculated by Klus et al. (2014) (which are roughly equivalent to using the reported outburst accretion rate and measured spin periods in equation 12). The cyan circles show the same data set using the accretion/ejection model and the time-averaged accretion rate, while the red squares show the same results for the trapped disc model. The black dashed line shows the quantum critical field, $B_{\rm crit} = 4.4 \times 10^{13}$G, where the cyclotron energy is comparable to the electron rest-mass energy, which is commonly used to define a 'magnetar'. Using the time-averaged accretion rate to estimate $B$ and assuming a trapped disc persists in quiescence obviates the need for magnetar-strength magnetic fields.

parameters. The resulting $P_{\rm eq}$ is $0.9P_{\rm eq,\,0}$[3] for a trapped disc, and $\sim 0.3P_{\rm eq,\,0}$ for the accretion/ejection model. The resulting estimated magnetic fields are shown in Fig. 22. As is clear from the figure, using a time-averaged accretion rate rather than the outburst one gives systematically lower estimates for $B$ regardless of the torque model, but if the systems are able to efficiently spin-down during quiescence (by transferring angular momentum into a disc), there is no need for the majority of systems to harbour magnetar-strength fields. Since the time-scales for reaching spin equilibrium in Be X-ray binaries are much shorter than for either TTauri stars or AMXPs, this result provides the strongest evidence for trapped discs around strongly magnetic stars.

### 5.3 Young stellar objects

TTauri stars also show strong evidence for spin regulation from interaction with an accretion disc (Bouvier et al. 2007), and most TTauri stars with discs spin well below their breakup rate, despite the fact that they contract as they evolve. The different mechanisms for angular momentum regulation discussed in this paper are thus relevant for these stars as well. TTauri stars are also often variable, showing variability on different time-scales. If the variability is caused by large accretion rate variations on to the stellar surface, then this should also affect the spin-equilibrium rate of the star, as discussed throughout this paper. TTauri stars are more similar to AMXPs than high-field NSs, with a much smaller magnetosphere that is probably completely crushed at high $\dot{M}$.

Since variability time-scales are much longer in TTauri stars than NSs, it is not straightforward to determine whether all TTauri stars

are variable. Recent work looking at variability has found that the most common variability – fluctuations on short time-scales (days to weeks) is most likely due to variations on the stellar surface that become apparent as the star rotates (Costigan et al. 2014). However, larger scale variability (which is observed in a subset of TTauri stars) *is* attributed to accretion rate fluctuations.

Variations of $\sim$10–100 with time-scales of a few years are seen in a subclass of TTauri stars known as 'EXors', after the prototype, EX Lupi (Herbig 2007). Even more dramatically, FU Ori-type stars undergo luminosity increases of $\sim 10^3$ times, and can persist for 50–100+ yr (Hartmann & Kenyon 1996). This paper is particularly relevant for these last two subtypes, since very large accretion rates should correspond to faster equilibrium spin rates. There is growing evidence that EXors are a distinct class (or alternately, evolutionary phase) of TTauri stars, so this phase may not generally last long enough to be relevant for long-term spin rates. In contrast, the long quiescent time-scales conjectured for FU Ori stars ($10^3$–$10^4$ yr) mean that most or all TTauri stars could pass through an extended FU Ori phase, which should then be reflected in the final spin rate.

Comparing the estimated $T_{\rm eq}$ for TTauri stars (see Table 1) with the predicted FU Ori outburst cycles shows another important distinction between TTauri stars and magnetic accreting compact objects: the duration of an outburst cycle is a much larger fraction (up to 10 per cent) of the nominal equilibrium time-scale (which as discussed could be much longer). As a result assuming spin equilibrium may not be valid.

Are the results of this paper consistent with observations of the spin rates of TTauri stars? Assuming that most stars go through enough FU Ori outbursts to reach spin equilibrium, the answer is sensitive to how the spin rate of the star is regulated. As seen in Section 4, when a simple 'accretion/ejection' picture is assumed, the star tends to spin-up to close to its outburst spin rate, rather than the long-term averaged one. For FU Ori stars, assuming a duty cycle of between 0.1 and 1 per cent, $\langle \dot{M} \rangle_{\rm out} \sim 10^{-4}$ $M_{\odot}$ yr$^{-1}$ versus $\langle \dot{M} \rangle \sim 10^{-7}$–$10^{-6}$ $M_{\odot}$ yr$^{-1}$. For a typical TTauri star, the accretion rate during outburst will be high enough to completely crush the magnetosphere, so that the disc accretes through a boundary layer directly on to the star. In standard accretion theory, the star should then spin-up to close to its breakup frequency (although see discussion below). The high outburst accretion rate will also presumably inhibit a magnetically driven wind from the stellar surface, which will limit how efficiently a wind can regulate the star's spin, and likely not be able to prevent the star from spinning up. Naïvely, one would then expect that TTauri stars in the FU Ori outburst stage should be spinning significantly faster than $P_{\rm eq}$ estimated from observations, which is most likely $\dot{M}$ in 'quiescence'. This does not immediately seem to be the case, although there may still be enough uncertainty in $B_*$ and the torque models that distinguishing between the two scenarios could be difficult.

In contrast, a trapped disc spins down the star in the quiescent state, and over time will bring the star into spin equilibrium with its long-term accretion rate. For a duty cycle of about 1 per cent, the accretion rate is still fairly high ($10^{-6} M_{\odot}$ yr$^{-1}$) and corresponds to a faster spin than is observed (0.5–1 d). If the duty cycle is shorter, the mean accretion rate can be close to the quiescent one ($10^{-7} M_{\odot}$ yr$^{-1}$), corresponding to a spin period of a few days, which is roughly consistent with observed spin periods.

These conclusions are also challenged by observational evidence that suggests the magnetosphere (Johnstone et al. 2014) and inner disc of young stars (Najita et al. 2007) are located well within $r_{\rm c}$. If these radius measurements are accurate it is somewhat surprising even within the 'standard' steady-state accretion model, since

---

[3] That is $P_{\rm eq}$ from equation (12).

it would suggest these stars are likely spinning up rapidly. It may indeed suggest enhanced spin-down torque at relatively high accretion rates (Zanni & Ferreira 2013). If most TTauri stars are FU Ors in quiescence, the problem is even larger: one would expect that the FU Ori events spin-up the star even more, requiring even stronger spin-down at lower accretion rates.

There are several other possibilities for reconciling the high FU Ori accretion rates with relatively long spin periods. One is that the FU Ori phase of repeated outbursts may only occur for a subset of TTauri stars, or that this accretion phase does not last long enough to bring the star into spin equilibrium. This question can only be resolved observationally. A second possibility is that accretion through a boundary layer does not easily spin the star up to breakup. This has been suggested in boundary layer calculations by Popham (1996) and more recently by new numerical and analytical work (Belyaev, Rafikov & Stone 2013). In the latter papers, the authors find that angular momentum and energy in the boundary layers are mainly transported via acoustic waves rather than an 'anomalous viscosity' as is typically assumed for both accretion discs and boundary layers. Belyaev et al. (2013) instead find angular momentum transport via waves can result in some outward transport (i.e. back into the disc), as well as into the deep layers of the star. Both these effects can limit how efficiently the star will spin-up, although by how much is not yet quantified.

However, without an additional very efficient and rapid source of angular momentum loss, the results here studying spin change in outbursts (both the expected final spin periods and the spin evolution time), combined with results suggesting most discs are truncated well within $r_c$, suggests that FU Ori phenomena are more likely a rare or brief evolutionary state, and most observed TTauri stars are not in the quiescent state of an FU Ori phase.

Finally, the conclusions from this section are somewhat preliminary, since the models of spin evolution adopted in this paper do not consider the radial contraction of the protostar during its lifetime, which will make the star spin faster and hence require even more angular momentum loss. While this is straightforward to include, it is outside the scope of the current paper.

## 5.4 Conclusions

The results of this paper suggest that the long-term spin evolution of magnetic stars can be significantly affected by large-scale changes in the mass accretion rate. In general, I find that by considering accretion outbursts, stars take significantly longer to reach their 'equilibrium' spin period and that this spin period in general can be significantly different (generally shorter, but not always) than would be predicted from simple analytic arguments. The $P_{eq}$ and $T_{eq}$ are sensitive to the disc–field interactions, the outburst duration, and the transport mechanism that removes angular momentum from the star.

In particular, the commonly envisioned scenario, in which gas either accretes on to the star or is expelled through a centrifugally launched wind, requires that the average accretion rate stay fairly steady in order to keep the star in near its predicted $P_{eq}$. This is because the spin-down mechanism is only efficient at relatively high $\dot{M}$ (when the inner disc remains close to $r_c$). Interestingly, this conclusion holds even for the more recent variants of this model, in which there is both accretion and ejection across a large range of $\dot{M}$ (Section 4.3). Such a steady $\dot{M}$ is inconsistent with the most widely accepted 'ionization instability' model for accretion outbursts, in which the accretion rate through the disc varies by several orders of magnitude between outburst and quiescence (Lasota 2001).

If a stellar wind (launched from the stellar surface but driven in part by accretion power) can be launched, spin-down can remain efficient as long as the mass outflow rate is high enough ($\sim 10$ per cent $\dot{M}$). There is some evidence supporting this idea for TTauri stars [e.g. Matt & Pudritz (2008) and other works by those authors], but the idea remains somewhat schematic and controversial (Zanni & Ferreira 2011), and the outflow rate from the star itself is difficult to constrain observationally. The 'trapped disc' model also has significant uncertainties, in particular the details of the coupling between the disc and the star, and the width of the coupled region (which sets the spin-down efficiency), but has the distinction of being able to spin-down the star very efficiently even at low $\dot{M}$. This could be very important in understanding the slow spin rates of Be X-ray binaries and possibly the long-term spin rates of millisecond pulsars.

In AMXPs, the large difference between outburst and quiescence means that accretion continues even when the cycle-averaged accretion rate is in the 'propeller' regime. This affects the conclusions of Tauris (2012), in particular, the assertion that AMXPs can efficiently spin-down via a propeller during a 'Roche lobe decoupling phase' (where the mean accretion rate drops rapidly). Observations indicate that AMXPs in general are *not* in spin equilibrium with $\langle \dot{M} \rangle$. This could support the conclusion that AMXPs are not the progenitor systems for the entire class of radio RMSP (Patruno & Watts 2012) and therefore that their faster average spin periods do not indicate a general spin evolution from one population to the other; alternately it could suggest that a trapped disc remains around the star even as $\langle \dot{M} \rangle$ drops and continues to spin the star down. Recent observations of transitional millisecond pulsar systems (Jaodand et al. 2016), however, suggest that the net spin-down from an accretion flow is comparable to that from dipole radiation.

In Be/X-ray binaries, considering the effects of outbursts changes the estimates of magnetic field (calculated assuming spin equilibrium) significantly. This conclusion applies even if an accretion/ejection model is considered, but it is especially true if a trapped disc remains present during quiescence. Considering these effects, the estimated magnetic field strengths for Be/X-ray binary systems (considering the large sample from the SMC, Coe et al. 2010) is significantly lower than estimated by Klus et al. (2014), and in particular does not require in magnetar-strength magnetic fields except for the slowest spinning stars.

It is not currently clear to what extent all protostars undergo repeated, large-scale outbursts, although at least a subset show large-scale variability. In these systems, the magnetosphere is likely crushed by accretion during the outburst, so that the star should accrete via a boundary layer. The outcome of this scenario is not completely clear, but naïvely one would expect that the final spin rate of the star would be dominated by what happens during outbursts (Popham 1996). Observations of the innermost regions of TTauri stars suggest that the inner disc and closed magnetosphere are generally well within $r_c$, indicating that these stars are more likely spinning *up* than spinning down after a large FU Ori-level outburst. This fact, and the fact that observed spin rates are generally much slower than breakup could then imply that either the star accretes without spinning up efficiently during outburst, or that FU Ori-type outbursts are not a universal or long-lasting phase of star formation. The results of this paper are preliminary though, since they do not include the contraction (and necessary spin-up) of the star as it evolves, nor spin regulation via boundary layer accretion.

**Note:** After this paper appeared on the arXiv, a similar work, focusing on transient accretion in AMXPs and considering only

an 'accretion/ejection' model was also published (Bhattacharyya & Chakrabarty [2017]). The authors conclude based on their analysis that gravitational waves may be required to prevent MSPs from spinning to submillisecond periods during outburst. They broadly reach the same conclusion as for the 'accretion/ejection' case considered here, namely, that stars should spin faster than predicted by the average accretion rate because a propeller outflow is generally inefficient, but do not find the same limit on spin period at the highest accretion rate (from limited spin-up efficiency because the source reaches $\dot{M}_{\rm Edd}$). Further investigation into what happens at high accretion rates is ongoing, and this will include a more detailed comparison with the results of that paper.

## REFERENCES

Alpar M. A., Cheng A. F., Ruderman M. A., Shaham J., 1982, Nature, 300, 728
Aly J. J., Kuijpers J., 1990, A&A, 227, 473
Andersson N., Kokkotas K. D., Stergioulas N., 1999, ApJ, 516, 307
Andersson N., Glampedakis K., Haskell B., Watts A. L., 2005, MNRAS, 361, 1153
Archibald A. M. et al., 2009, Science, 324, 1411
Audard M. et al., 2014, Protostars and Planets VI. Univ. Arizona, Tucson, AZ, p. 387
Bachetti M. et al., 2014, Nature, 514, 202
Bassa C. G. et al., 2014, MNRAS, 441, 1825
Belyaev M. A., Rafikov R. R., Stone J. M., 2013, ApJ, 770, 67
Bessolaz N., Zanni C., Ferreira J., Keppens R., Bouvier J., 2008, A&A, 478, 155
Bhattacharyya S., Chakrabarty D., 2017, ApJ, 835, 4
Bildsten L., 1998, ApJ, 501, L89
Bildsten L. et al., 1997, ApJS, 113, 367
Bouvier J., Alencar S. H. P., Harries T. J., Johns-Krull C. M., Romanova M. M., 2007, Protostars and Planets V. Univ. Arizona, Tucson, AZ, p. 479
Cauley P. W., Johns-Krull C. M., Hamilton C. M., Lockhart K., 2012, ApJ, 756, 68
Chakrabarty D., Morgan E. H., Muno M. P., Galloway D. K., Wijnands R., van der Klis M., Markwardt C. B., 2003, Nature, 424, 42
Coe M., Corbet R. H. D., McGowan K. E., McBride V. A., 2010, in Martí J., Luque-Escamilla P. L., Combi J. A., eds, ASP Conf. Ser. Vol. 422, High Energy Phenomena in Massive Stars. Astron. Soc. Pac., San Francisco, p. 224
Costigan G., Vink J. S., Scholz A., Ray T., Testi L., 2014, MNRAS, 440, 3444
D'Angelo C. R., Spruit H. C., 2010, MNRAS, 406, 1208
D'Angelo C. R., Spruit H. C., 2011, MNRAS, 416, 893
D'Angelo C. R., Spruit H. C., 2012, MNRAS, 420, 416
D'Angelo C. R., Fridriksson J. K., Messenger C., Patruno A., 2015, MNRAS, 449, 2803
Frank J., King A., Raine D. J., 2002, Accretion Power in Astrophysics. Cambridge Univ. Press, Cambridge
Fürst F. et al., 2016, ApJ, 831, L14
Ghosh P., Lamb F. K., 1979, ApJ, 232, 259
Ghosh P., Pethick C. J., Lamb F. K., 1977, ApJ, 217, 578
Goodson A. P., Winglee R. M., Boehm K., 1997, ApJ, 489, 199
Hartmann L., Kenyon S. J., 1996, ARA&A, 34, 207
Hayashi M. R., Shibata K., Matsumoto R., 1996, ApJ, 468, L37+
Herbig G. H., 2007, AJ, 133, 2679
Hessels J. W. T., Ransom S. M., Stairs I. H., Freire P. C. C., Kaspi V. M., Camilo F., 2006, Science, 311, 1901
Hillenbrand L. A., Findeisen K. P., 2015, ApJ, 808, 68
Ho W. C. G., Klus H., Coe M. J., Andersson N., 2014, MNRAS, 437, 3664
Jaodand A., Archibald A. M., Hessels J. W. T., Bogdanov S., D'Angelo C. R., Patruno A., Bassa C., Deller A. T., 2016, ApJ, 830, 122
Johnstone C. P., Jardine M., Gregory S. G., Donati J.-F., Hussain G., 2014, MNRAS, 437, 3202
Klus H., Ho W. C. G., Coe M. J., Corbet R. H. D., Townsend L. J., 2014, MNRAS, 437, 3863
Kluźniak W., Rappaport S., 2007, ApJ, 671, 1990
Lai D., 2014, in Bozzo E., Kretschmar P., Audard M., Falanga M., Ferrigno C., eds, European Physical Journal Web of Conferences. EDP Sciences, France, p. 01001
Lasota J., 2001, New Astron. Rev., 45, 449
Lii P. S., Romanova M. M., Ustyugova G. V., Koldoba A. V., Lovelace R. V. E., 2014, MNRAS, 441, 86
Lovelace R. V. E., Romanova M. M., Bisnovatyi-Kogan G. S., 1995, MNRAS, 275, 244
Matt S., Pudritz R. E., 2005, ApJ, 632, L135
Matt S., Pudritz R. E., 2008, ApJ, 681, 391
Messenger C., Patruno A., 2015, ApJ, 806, 261
Miller K. A., Stone J. M., 1997, ApJ, 489, 890
Najita J. R., Carr J. S., Glassgold A. E., Valenti J. A., 2007, Protostars and Planets V. Univ. Arizona Press, Tucson, AZ, p. 507
Narayan R., Yi I., 1994, ApJ, 428, L13
Paczynski B., 1991, ApJ, 370, 597
Papitto A. et al., 2013, Nature, 501, 517
Papitto A., Torres D. F., Rea N., Tauris T. M., 2014, A&A, 566, A64
Patruno A., Watts A. L., 2012, preprint (arXiv:1206.2727)
Patruno A., Haskell B., D'Angelo C., 2012, ApJ, 746, 9
Popham R., 1996, ApJ, 467, 749
Popham R., Narayan R., 1991, ApJ, 370, 604
Pringle J. E., Rees M. J., 1972, A&A, 21, 1
Reig P., 2011, Ap&SS, 332, 1
Romanova M. M., Toropina O. D., Toropin Y. M., Lovelace R. V. E., 2003, ApJ, 588, 400
Shakura N. I., Sunyaev R. A., 1973, A&A, 24, 337
Spruit H. C., Taam R. E., 1993, ApJ, 402, 593
Sugizaki M., Mihara T., Nakajima M., Yamaoka K., 2015, preprint (arXiv:1502.04461)
Sunyaev R. A., Shakura N. I., 1977, Pis'ma Astron. Zh., 3, 262
Tauris T. M., 2012, Science, 335, 561
Uzdensky D. A., 2004, Ap&SS, 292, 573
Wang Y.-M., 1987, A&A, 183, 257
Wang Y.-M., 1996, ApJ, 465, L111
Watts A. L., Krishnan B., Bildsten L., Schutz B. F., 2008, MNRAS, 389, 839
Yan Z., Yu W., 2015, ApJ, 805, 87
Zanni C., Ferreira J., 2011, ApJ, 727, L22
Zanni C., Ferreira J., 2013, A&A, 550, A99

This paper has been typeset from a TeX/LaTeX file prepared by the author.